

# Inertial and coriolis effects on oscillatory flow in a horizontal dendrite layer

D. N. Riahi

Received: 2 January 2006 / Accepted: 12 October 2006 / Published online: 22 March 2007  
© Springer Science+Business Media B.V. 2007

**Abstract** Flow instability due to oscillatory modes of disturbances in a horizontal dendrite layer during alloy solidification is investigated under an external constraint of rotation. The flow in the dendrite layer, which is modeled as flow in a porous layer and with the inertial effects included, is assumed to rotate about the vertical axis at a constant angular velocity. The investigation is an extension of the work in Riahi (On stationary and oscillatory modes of flow instability in a rotating porous layer during alloy solidification. *J. Porous Media*, **6**, 177–187, 2003), which was for the case in the absence of the inertial effects. Results of the stability analyses indicate, in particular, that the Coriolis effect can enhance the physical domain for the oscillatory flow, while the inertial effect tends to reduce such domain. Sufficiently strong inertial effect can eliminate presence of the oscillatory mode only for the rotation rate beyond some value. The effect of interaction between the local volume fraction of solid and the flow associated with the Coriolis term was found to be stabilizing.

**Keywords** Rotating convection · Dendrite layer · Solidification · Oscillatory convection · Oscillatory instability · Inertial flow · Mushy layers · Stability analysis

## Nomenclature

### *Latin symbols*

$a$	Horizontal wave number	$\mathbf{a}$	Horizontal wave number vector
$a_1$	$x$ -Component of $\mathbf{a}$	$a_2$	$y$ -Component of $\mathbf{a}$
$a_c$	Critical $a$	$C$	Scaled concentration ratio
$\tilde{C}$	Dimensional composition	$C_0$	Far field composition
$C_e$	Eutectic composition	$C_l$	Specific heat per unit volume
$C_r$	A concentration ratio	$C_s$	Composition of dendrites
$d$	Dendrite layer thickness	$g$	Acceleration due to gravity

---

D. N. Riahi (✉)  
Department of Mathematics, University of Texas-Pan American,  
1201 W. University Dr., Edinburg, Texas 78541-2999, USA  
e-mail: riahid@aol.com

$G$	$1 + S/C$	$G_t$	$(G - 1)/(CG^2)$
$i$	Pure imaginary number	$K$	A permeability reciprocal
$K_1$	A permeability parameter	$k$	Thermal diffusivity
$k_s$	Solute diffusivity	$L$	An inertial parameter
$L_a$	Latent heat of solidification	$\tilde{L}$	An inertial parameter
$M$	Liquidus slope	$P$	Scaled modified pressure
$\tilde{P}$	Modified pressure	$P_0$	A constant
$P_B$	Modified basic pressure	$Q$	Rotation rate
$R$	Scaled Rayleigh number	$\tilde{R}$	Rayleigh number
$R_c$	Critical $R$	$S$	Scaled Stefan number
$S_t$	Stefan number	$t$	Scaled time variable
$T$	Coriolis parameter	$\tilde{t}$	Time variable
$T_e$	Eutectic temperature	$T_L$	Liquidus temperature
$T_\infty$	Far field temperature	$\mathbf{u}$	Scaled Darcy's velocity vector
$\mathbf{U}$	Velocity vector	$\tilde{\mathbf{u}}$	Darcy's velocity vector
$\tilde{u}$	$x$ -Component of $\mathbf{u}$	$W$	Poloidal function for $\mathbf{u}$
$V$	Solidification speed		
$\tilde{v}$	$y$ -Component of $\mathbf{u}$	$\tilde{w}$	$z$ -Component of $\mathbf{u}$
$x$	A scaled horizontal variable	$\mathbf{x}$	Unit vector along $x$ -axis
$\tilde{x}$	A horizontal variable	$y$	A scaled horizontal variable
$\mathbf{y}$	Unit vector along $y$ -axis	$\tilde{y}$	Another horizontal variable
$z$	Scaled vertical variable	$\mathbf{z}$	Unit vector along $z$ -axis
$\tilde{z}$	Vertical variable		
<i>Greek symbols</i>			
$\alpha^*$	Thermal expansion coefficient	$\beta^*$	Solute expansion coefficient
$\beta$	$\beta^* - M\alpha^*$	$\Delta C$	$C_0 - C_e$
$\Delta T$	$T_L(C_0) - T_e$	$\Delta$	Horizontal Laplacian operator
$\delta$	Dimensionless depth of the porous layer	$\nabla$	Gradient operator
$\tilde{\theta}$	Temperature	$\theta_B$	Basic temperature
$\theta$	Perturbation Temperature	$\theta_\infty$	$T_\infty/\Delta T$
$\nu$	Kinematic viscosity	$\Pi$	Permeability
$\Pi(0)$	A reference permeability	$\phi$	Perturbation to solid fraction
$\phi_B$	Basic solid fraction	$\tilde{\phi}$	Local volume fraction of solid
$\rho_0$	A reference density	$\sigma$	Complex growth rate of disturbance
$\sigma_i$	Disturbance frequency	$\sigma_r$	Real growth rate of disturbance
$\psi$	Toroidal function for $\mathbf{u}$		

## 1 Introduction

The problem studied in this paper and in Riahi (2003), which is hereafter referred to as R03, is based on the conditions considered by Anderson and Worster (1996) who studied the problem of the solidification of a binary alloy in a mushy layer, which was treated as a porous layer, and analyzed the linear stability of a motionless state to identify an oscillatory convective mode of instability. Their system was under no rotational constraint, and their investigation was based on the earlier mushy-layer model of Amberg and Homsy (1993). A near-eutectic approximation was employed

and the limit of large far-field temperature was considered. Such asymptotic limits allowed them to examine the dynamics of the mushy layer in the form of small deviation from the classical system of convection in a horizontal porous layer of constant permeability. They also considered the limit of large Stefan number, which enabled them to reach a domain for the existence of the oscillatory instability.

Recently R03 extended the linear model treated by Anderson and Worster (1996) by taking into account the effect of rotation due to the Coriolis-force term in the momentum-Darcy equation and examined presence of oscillatory mode versus the stationary mode, and he obtained some new results. Similar to the work in Anderson and Worster (1996), it was assumed that inertial terms in the momentum-Darcy equation were negligibly small and, thus, the effects of such terms were totally discarded. The expressions for various quantities were found to be affected by the presence of rotation and certain new qualitative results due to the rotational effect were reported. For example, in the presence of rotation it was found that, in contrast to the stationary mode, the most critical oscillatory mode may be able to reduce the tendency for the chimney formation in the mushy layer. Information about chimney formation can be important in the industrial crystal growth processes where it is of interest to find ways to reduce the undesirable effects of the chimney convection during the alloy solidification since presence of chimney convection is known to lead to imperfections in the final produced crystals, which can significantly reduce the quality of the solidified materials.

The only other studies on oscillatory convection in a rotating dendrite layer are those due to Guba and Boda (1998) and Govender and Vadasz (2002). Guba and Boda (1998) studied the effect of rotation on the linear problem of convection in the absence of inertia effects in a dendrite layer during the directional solidification of a binary alloy, where such layer often is referred to in this area as a mushy layer, and their investigation also did not take into account the interaction between the local volume fraction of solid and the flow associated with the Coriolis term. Their main result was that depending on the values of the parameters, the oscillatory mode could be more critical than the stationary mode or vice versa. Govender and Vadasz (2002) considered the problem of two-dimensional oscillatory convection in a rotating mushy layer. The momentum-Darcy equation was extended only to include the time derivative and the Coriolis terms. The authors did not take into account the presence of the interactions between the local solid fraction and the flow associated with the Coriolis term, and their weakly nonlinear analysis was based on the zero-order limit of the mushy-layer thickness. The main result of the study was that two-dimensional oscillatory flow was supercritical.

In the present paper we consider the linear problem for the dendrite system again under the external constraint of rotation, and we examine the properties of the oscillatory mode further by including the interaction between the local solid fraction and the flow associated with the Coriolis term and following Vadasz (1998) to include the time-derivative inertial term in the momentum-Darcy equation. Due to the linearity and the zero-basic volume flux of the present problem (R03), the nonlinear inertial term has no contribution in the momentum-Darcy equation even if the nonlinear inertial terms have not been discarded in the full non-linear system. We find some interesting results about the effects of inertial and Coriolis terms on the oscillatory mode. In particular, we find that the presence of the inertial term can have significant effects on the existence of the oscillatory mode or on the value of the period of oscillation of such mode, and rotation effect can enhance such effects. However,

rotational effect can also have an opposing effect in the sense that it enhances the domain of the oscillatory mode, while the inertial effect reduces such domain. The effect of interaction between the local solid fraction and the flow associated with the Coriolis term was found to be stabilizing.

In regard to the motivation of the present study and the applicability of the present results, understanding the rotational effects on the convective flow instabilities in the dendrite layer, which can be formed adjacent to the crystal interface in an alloy system where the inertial effects are not negligible (Vadasz 1998), are of interest in both geophysical and engineering areas. Understanding the roles and effects of the Coriolis force on the dynamics of a porous layer adjacent to the earth's inner core interface is important in geophysics and for understanding the geodynamo. In industrial crystal growth processes it has been desirable to impose certain external constraints such as rotation, in an optimized manner upon the system, in order to reduce the effects of such instabilities, which can lead to micro-defect density in the crystal and, thus, reduce the quality of the produced crystal.

It should be noted that the model considered in R03 as well as the present one, which takes into account the rotational effects through the presence of the Coriolis force only, is relevant both in the geophysical applications where the centrifugal mode of convection is insignificant and in the engineering areas where the neglect of the centrifugal effect can be justified under the present assumption that the gravitational buoyancy is much larger than the centrifugal force.

## 2 Formulation and analysis

The formulation and analysis are presented briefly here since, apart from the inertial contributions, they are basically of the same types presented in R03, and, thus, the reader is referred to R03 for details.

We consider a binary alloy melt that is cooled from below and is solidified at a constant speed  $V$ . The solidifying system is assumed to be rotating at a constant speed  $Q$  about the vertical direction, anti-parallel to the gravity vector (Fig. 1). Following Amberg and Homsy (1993) and Anderson and Worster (1996), we consider the dendrite layer of thickness  $d$  adjacent and above the solidification front to be physically isolated from the overlying liquid and the underlying solid zones. The overlying liquid is assumed to have a composition  $C_0 > C_e$  and a temperature  $T_\infty > T_L(C_0)$  far above the mushy layer, where  $C_e$  is the eutectic composition,  $T_L(\tilde{C})$  is the liquidus temperature of the alloy and  $\tilde{C}$  is the composition. Thus, it is assumed that the horizontal mushy layer, which is treated as a porous layer, is bounded from above and below by

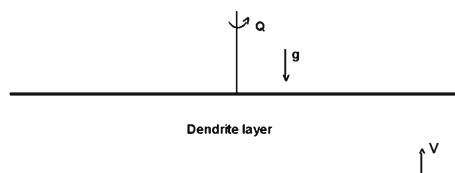


**Fig. 1** A diagram representing the physical system under consideration. A dendrite layer is solidified from below at a constant speed  $V$  and is rotating at a constant rate  $Q$  about the vertical direction, anti-parallel to the gravity vector

rigid and isothermal boundaries. We consider the solidification system in a moving frame of reference  $o\tilde{x}\tilde{y}\tilde{z}$ , whose origin lies on the solidification front, translating at the speed  $V$  with the solidification front in the positive  $\tilde{z}$ -direction and rotating with the speed  $Q$  about the  $\tilde{z}$ -axis.

Next, we consider the equations for extended Darcy-momentum to include the time derivative and Coriolis terms, continuity, heat, and solute for the flow in the mushy layer in the moving frame. The equations are non-dimensionalized by using  $V, k/V, k/V^2, \beta\Delta C\rho_0gk/V, \Delta C,$  and  $\Delta T$  as scaled for velocity, length, time, pressure, solute, and temperature, respectively. Here  $k$  is the thermal diffusivity,  $\rho_0$  is a reference (constant) density,  $\beta = \beta^* - M^*, \alpha^*,$  and  $\beta^*$  are the expansion coefficients for the heat and solute respectively and the slope of liquidus  $M$  is assumed to be constant,  $\Delta C = C_0 - C_e, \Delta T = T_L(C_0) - T_e,$  and  $T_e$  is the eutectic temperature. The non-dimensional form of the equations for extended Darcy-momentum, continuity, temperature and solute concentration, under the Boussinesq approximation (Chandrasekhar 1961), in the mushy layer are

$$\{[\tilde{L}/(1 - \tilde{\phi})](\partial/\partial\tilde{t} - \partial/\partial\tilde{z}) + K(\tilde{\phi})\}\tilde{\mathbf{u}} = -\nabla\tilde{P} - \tilde{R}\tilde{\theta}\mathbf{z} + T\tilde{\mathbf{u}} \times \mathbf{z}/(1 - \tilde{\phi}), \tag{1a}$$

$$\nabla \cdot \tilde{\mathbf{u}} = 0, \tag{1b}$$

$$(\partial/\partial\tilde{t} - \partial/\partial\tilde{z})(\tilde{\theta} - S_t\tilde{\phi}) + \tilde{\mathbf{u}} \cdot \nabla\tilde{\theta} = \nabla^2\tilde{\theta}, \tag{1c}$$

$$(\partial/\partial\tilde{t} - \partial/\partial\tilde{z})[(1 - \tilde{\phi})\tilde{\theta} + C_r\tilde{\phi}] + \tilde{\mathbf{u}} \cdot \nabla\tilde{\theta} = 0, \tag{1d}$$

where no change of volume upon change of phase is assumed (Worster 1991). Here  $\tilde{\mathbf{u}} = \tilde{u}\mathbf{x} + \tilde{v}\mathbf{y} + \tilde{w}\mathbf{z} = (1 - \tilde{\phi})\mathbf{U}$  is the volume flux vector per unit area (Worster 1992), which is also known as Darcy’s velocity vector,  $\mathbf{U}$  is velocity vector,  $\tilde{u}$  and  $\tilde{v}$  are the horizontal components of  $\tilde{\mathbf{u}}$  along the  $\tilde{x}$ - and  $\tilde{y}$ -directions, respectively,  $\mathbf{x}$  and  $\mathbf{y}$  are unit vectors along the positive  $\tilde{x}$ - and  $\tilde{y}$ -directions,  $\tilde{w}$  is the vertical component of  $\tilde{\mathbf{u}}$  along the  $\tilde{z}$ -direction,  $\mathbf{z}$  is a unit vector along the positive  $\tilde{z}$ -direction,  $\tilde{P}$  is the modified pressure,  $\tilde{\theta}$  is the non-dimensional composition (or equivalently temperature),  $\tilde{\theta} = [\tilde{T} - T_L(C_0)]/\Delta T = (\tilde{C} - C_0)/\Delta C, \tilde{t}$  is the time variable,  $\tilde{\phi}$  is the local solid fraction,  $\tilde{R} = \beta\Delta Cg\Pi(0)/(V\nu)$  is the Rayleigh number,  $\Pi(0)$  is reference value at  $\tilde{\phi} = 0$  of the permeability  $\Pi(\tilde{\phi})$  of the porous medium,  $\nu$  is the kinematic viscosity,  $g$  is acceleration due to gravity,  $K(\tilde{\phi}) \equiv \Pi(0)/\Pi(\tilde{\phi}), S_t = L_a/(C_l\Delta T)$  is the Stefan number,  $C_l$  is the specific heat per unit volume,  $L_a$  is the latent heat of solidification per unit volume,  $C_r = (C_s - C_0)/\Delta C$  is a concentration ratio,  $C_s$  is the composition of the solid-phase forming the dendrites,  $\tilde{L} = V^2\Pi(0)/(k\nu)$  is an Inertial type of parameter and  $T = 2Q\Pi(0)/\nu$  is the Coriolis parameter.

The boundary conditions are

$$\tilde{\theta} + 1 = \tilde{w} = 0 \quad \text{at} \quad z = 0, \tag{2a}$$

$$\tilde{\theta} = \tilde{w} = \tilde{\phi} = 0 \quad \text{at} \quad z = \delta, \tag{2b}$$

where  $\delta = dV_0/k$  is the dimensionless depth of the layer.

We now assume the following rescaling in the limit of sufficiently small  $\delta$ :

$$C_r = C/\delta, S_t = S/\delta, L = \tilde{L}/\delta^2, \delta \ll 1, \tag{3a}$$

$$(\tilde{x}, \tilde{y}, \tilde{z}) = \delta(x, y, z), \tilde{t} = \delta^2t, R^2 = \delta\tilde{R}, \tag{3b}$$

$$\tilde{\mathbf{u}} = R\mathbf{u}/\delta, \tilde{P} = RP, \tag{3c}$$

where  $C$  and  $S$  are order one quantities as  $\delta \rightarrow 0$ .

The rescaling (3a)–(3c) are then used in (1a)–(1d) and (2a)–(2b). The resulting system of equations and boundary conditions admits a motionless basic state, which is steady and horizontally uniform. The basic state solution, denoted by subscript ‘B’ is the same as the one given in R03 and will not be repeated here. Since  $\phi_B \ll 1$  (R03) and, thus,  $\tilde{\phi}$  is expected to be small, the following expansion for  $K(\tilde{\phi})$  is implemented in the governing system:

$$K(\tilde{\phi}) = 1 + K_1\tilde{\phi} + K_2\tilde{\phi}^2 + \dots, \tag{4}$$

where the coefficients  $K_1$  and  $K_2$  are constants.

For the analysis to be described briefly next, it was found convenient to use the representation

$$\mathbf{u} = \nabla \times (\nabla \times \mathbf{z}W) + \nabla \times \mathbf{z}\psi \tag{5}$$

for the vector field  $\mathbf{u}$  (Chandrasekhar 1961) of the infinitesimal disturbances superimposed on the motionless basic state, where  $W$  and  $\psi$  are the poloidal and toroidal functions for the disturbance vector  $\mathbf{u}$ , respectively, and  $W = 0$  at the top and bottom boundaries of the layer. Taking the vertical components of the curl and the double-curl of the Darcy-momentum equation (1a) and using the basic state solution and (3)–(5) in (1)–(2), we find the leading order system for the dependent variables  $W, \psi, \theta$ , and  $\phi$  of the infinitesimal disturbances, where  $(\theta, \phi) = (\tilde{\theta} - \theta_B, \tilde{\phi} - \phi_B)$ .

We now seek normal mode type solution of the form

$$(W, \psi, \theta, \phi) = [W'(z), \psi'(z), \theta'(z), \phi'(z)] \exp(\sigma t + i\mathbf{a}\cdot\mathbf{r}), \tag{6}$$

where  $\sigma = \sigma_r + i\sigma_i$  is the complex growth rate,  $i$  is the pure imaginary number ( $\sqrt{-1}$ ),  $\sigma_r$  is the real growth rate,  $\sigma_i$  is the frequency of the disturbances,  $\mathbf{r} = (x, y)$  is the horizontal position vector and  $\mathbf{a} = (a_1, a_2)$  is the horizontal wave number vector of the disturbances. Here  $a_1$  and  $a_2$  are the  $x$  and  $y$  components of  $\mathbf{a}$ , respectively. Using (6) in the governing system, we find a system of ordinary differential equations and boundary conditions for the  $z$ -dependent coefficients  $W', \psi', \theta'$ , and  $\phi'$ .

Next, presence of small parameter  $\delta$  in the system for the  $z$ -dependent coefficients suggests the following expansions of the dependent variables and parameters in powers of  $\delta$ :

$$(W', \psi', \theta', \phi', R, \sigma_r, \sigma_i) = (w_0, \psi_0, \theta_0, \phi_0, R_0, \sigma_{r0}, \sigma_{i0}) + \delta(w_1, \psi_1, \theta_1, \phi_1, R_1, \sigma_{r1}, \sigma_{i1}) + \dots \tag{7}$$

Using (7) in the system for the  $z$ -dependent coefficients, we solve the resulting systems in the orders  $1/\delta, \delta^0$ , and  $\delta^1$  to determine the main stability results.

At order  $1/\delta$  we find

$$\sigma_{r0} = \sigma_{i0} = 0 \tag{8}$$

At order  $\delta^0$  we find the leading order eigensolutions to be the same as those given in R03 and will not be repeated here. In addition, we find

$$R_0^2 = (\pi^2 + a^2)[(\pi^2 + a^2) + \pi^2 T^2]/(a^2 G), \tag{9}$$

where  $a = |\mathbf{a}|$ .

If we restrict ourselves to the solutions up to and including order  $\delta^0$ , then  $R_0$  is minimized with respect to  $a$  to yield

$$R_{0c} = \pi[1 + (1 + T^2)^{1/2}]/\sqrt{G}, \tag{10a}$$

$$a_{0c} = \pi(1 + T^2)^{1/4}, \tag{10b}$$

where  $G = S/C+1$  and  $R_{0c}$  is the minimum value of  $R_0$  achieved at  $a = a_{0c}$ .

At order  $\delta$  we find the simplified system for  $w_1$  and  $\theta_1$  after eliminating  $\psi_1$  and  $\phi_1$  between all the four equations. We then multiply the equation for  $w_1$  by  $Ga^2w_0$  and the equation for  $\theta_1$  by  $\theta_0$ , add the resulting equations, integrate over the fluid layer and make use of the boundary conditions. The result is a complex equation whose real and imaginary parts for the neutrally stable flow case, where  $\sigma_{r1} = 0$ , yield

$$\begin{aligned} (R_1/R_0) = & [K_1/(4C)][(\pi^2 + a^2 - \pi^2T^2)/(\pi^2 + a^2 + \pi^2T^2)] \\ & + \pi^2T^2/[2C(\pi^2 + a^2 + \pi^2T^2)] + GG_t\{1/4 + \pi^2[1 + \cos(\sigma_{i1})]/(\pi^2 - \sigma_{i1}^2)^2\}, \end{aligned} \tag{11a}$$

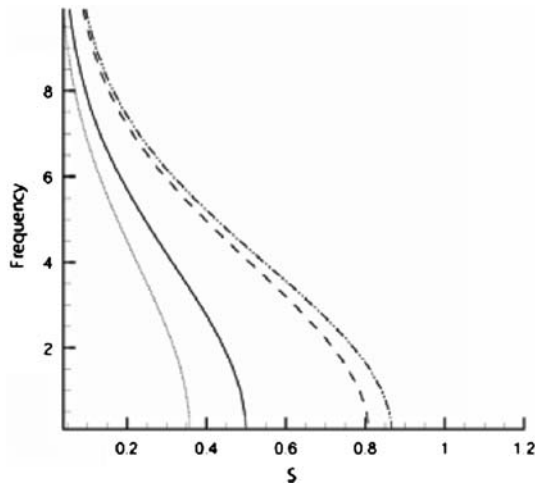
$$\begin{aligned} \sigma_{i1}\{1 + G_t[(\pi^2 + a^2)/(\pi^2 - \sigma_{i1}^2)]\}[1 - 2\pi^2\sin\sigma_{i1}/(\sigma_{i1}\pi^2 - \sigma_{i1}^3)] + \\ L(\pi^2 + a^2)^2[\pi^2(1 - T^2) + a^2]/(R_0Ga)^2 = 0, \end{aligned} \tag{11b}$$

where  $G_t = (G - 1)/(CG^2)$ . The expressions for  $w_1$ ,  $\psi_1$ ,  $\theta_1$ , and  $\phi_1$  are generally lengthy and will not be given here.

### 3 Results and discussion

It can be seen from the Eq. (11b) that zero value of the frequency is always a solution of this equation, so that stationary mode of neutrally stable state is always a solution to the present problem. However, stationary solution does not carry the effect of the inertial term in the present problem since such inertial term is due to the time derivative term in the momentum-Darcy equation and vanishes for any stationary mode of the problem. To investigate the possibility for oscillatory instability, we need to look for solutions with non-zero frequency of (11b). In most of our presentation of the results in the present problem, we consider the dependence of the solutions based on the physical parameters  $S$  and  $C$  rather than on the composite parameters  $G$  and  $G_t$ . Figure 2 presents the magnitude of the frequency of the critical oscillatory mode versus  $S$  in the neutrally stable regime, which corresponds to the lowest value of  $R$ , for  $C = S$ . Here the solid line, dotted line, dashed line, and dash-dot-dot line correspond, respectively, to  $T = L = 0$ ,  $T = L - 0.04 = 0$ ,  $T - 2 = L = 0$ , and  $T - 2 = L - 0.04 = 0$ . The values of the magnitude of the frequency are independent with respect to  $G$  as can be seen from (11b). It can be seen from this figure that for  $T = 0$  the value of the magnitude of the frequency is smaller for  $L = 0.04$  as compared with the one for  $L = 0$ , while for  $T = 2$  the value of such magnitude is larger for  $L = 0.04$  as compared with the one for  $L = 0$ . The results of our more generated data for the frequency indicate that the higher value of the period of oscillation of the solution corresponds to the case with non-zero inertial effect if the rotation rate is sufficiently small, while the smaller period of oscillation corresponds to the case with non-zero inertial effect if the rotation rate is sufficiently large. In addition, we find that non-zero frequency is possible for all values of  $L$  only if  $T$  is sufficiently

**Fig. 2** Frequency versus  $S$  for  $C = S$ . Here solid line, dashed line, dotted line, and dash-dot-dot line present, respectively, the cases of  $T = L = 0$ ,  $T - 2 = L = 0$ ,  $T = L - 0.04 = 0$ , and  $T - 2 = L - 0.04 = 0$



small. However, if, for example,  $L \geq 0.1$ , then no non-zero value of the frequency is possible for  $T \geq 4$ . Rotation was found to enhance the domain in  $(S, C)$ -plane for the oscillatory mode, while inertial effect reduces such domain. It should be noted that throughout this paper by the oscillatory mode we mean one that was detected first by Anderson and Worster (1996) in the absence of rotation and inertial effects.

As can be seen from (11b), both  $+\sigma_{i1}$  and  $-\sigma_{i1}$  are two solutions to the equation (11b) which correspond to the same value for  $R_1$  as can be found from (11a). These two modes are neutrally stable at the critical value  $R_c$  of the Rayleigh number. To determine further the properties of the oscillatory mode at the onset of convection, we need to examine the expression for  $R_c$  given by

$$R_c = R_{0c} + \delta R_{1c} + O(\delta^2), \tag{12}$$

where  $R_{0c}$  is given by (10a), and  $R_{1c}$  is given by (11a), provided  $R_0$ ,  $a$  and  $\sigma_{i1}$  are replaced, respectively, by  $R_{0c}$ , given by (10a),  $a_{0c}$ , given by (10b), and  $\sigma_{i1}$  corresponding to the value  $R = R_c$ . It should be noted that in the expression (11a) for  $R_1$ , the second term in the right-hand-side, which contains the factor  $(T^2/C)$ , is due to the interaction between the leading term in the basic state of the local solid fraction and the Coriolis term in the momentum-Darcy equation. If this interaction term is not taken into account, then we found that the value of  $R$  is reduced for the non-zero rotation case. Hence, presence of such interaction is stabilizing for the oscillatory flow in the linear regime.

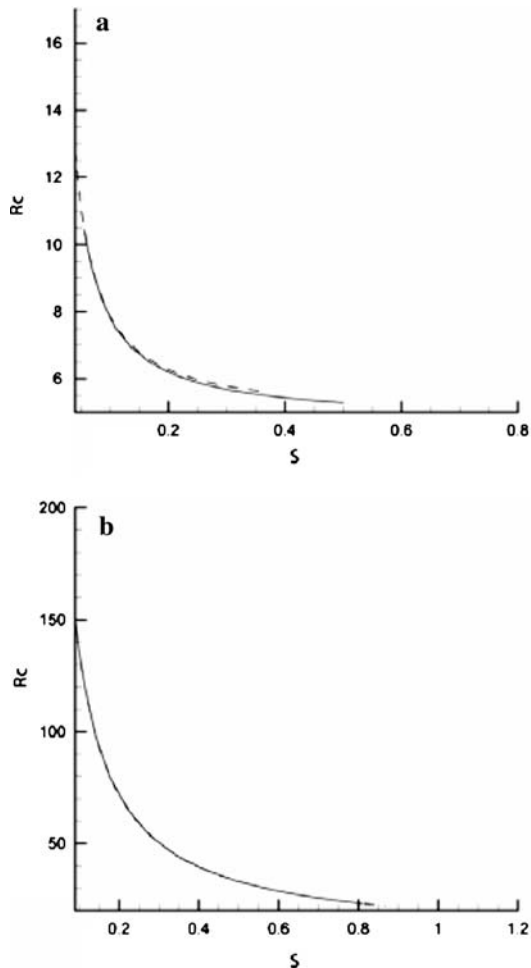
It can be seen from (10a), (11a), and (12) that the dependence of  $R_c$  on  $L$  is only indirectly through the dependence of the frequency on  $L$ . Figures 3a and 3b present  $R_c$  versus  $S$  for  $T = 0$  and  $T = 2$ , respectively, and for  $C = S$ ,  $K_1 = 1.0$  and two different values of  $L$ . In each figure solid line corresponds to the case  $L = 0$  and the dashed line corresponds to  $L = 0.04$ . Both figures are drawn for the same values of the frequency in the range  $0.1 \leq \sigma_{i1} \leq 9.90$ . It can be seen from both figures that rotation is stabilizing, while the flow destabilizes as  $S$  increases. Since  $S$  represents a measure of the latent heat relative to the heat content and  $C$  represents a measure of the difference in the characteristic composition of the solid-dendrite and liquid phases to the compositional variation of the liquid, the system is expected to destabilize as



$S$  increases or as  $C$  decreases. However, for the present case where  $C = S$ , it should be concluded that the destabilizing effect of  $S$  dominates over the stabilizing effect of  $C$  in the present problem. Although it cannot be seen much difference between cases  $L = 0$  and  $L = 0.004$  for  $T = 0$  and 2 from the Fig. 3a, b, the numerical values of the corresponding data indicated the following features. For  $T = 0$ , the inertial effect is slightly stabilizing especially for larger values of  $S$ , and it also tends to reduce the domain for the oscillatory mode. For  $T = 2$ , the stabilizing effect of the inertial force is neutralized by the effect of rotation, while reduction of the oscillatory domain is increased further by the inertial force in the presence of rotation.

The results (10a) and (10b) for  $R_{0c}$  and  $a_{0c}$  and the fact that the critical values  $R_c$  and  $a_c$  for  $R$  and  $a$  can be in a small neighborhood about  $R_{0c}$  and  $a_{0c}$ , respectively, due to small deviation of  $R_0$  from  $R$ , indicate that the critical values  $R_c$  and  $a_c$  increase with  $T$ . Hence, presence of the rotational constraint exerts stabilizing effect on the oscillatory mode at the onset of convection since  $R_{0c}$  increases with  $T$ . Also, the rotational

**Fig. 3** (a)  $R_c$  versus  $S$  for  $C = S, K_1 = 1$ , and  $T = 0$ . Here solid and dashed lines present, respectively, the cases of  $L = 0$  and 0.04. (b) The same as in the (a) but for  $T=2$



constraint through the Coriolis force reduces the wavelength of the preferred flow since  $a_c$  increases with  $T$ .

We also examined the vertical distribution of the perturbation to the solid fraction  $\phi = [\phi_0 + \delta\phi_1 + O(\delta^2)]$  for the oscillatory mode at  $C = S$ . Some results are presented in Fig. 4 for the vertical distribution of the perturbation to the solid fraction, which can provide information for the tendency for chimney formation in the mushy zone if the value of  $\phi$  is negative, while tendency for the enhancement of the solid structure in the porous medium follows if the value of  $\phi$  is positive. For this figure,  $\delta = 0.2$ ,  $K_1 = 1.0$  and the value of 0.01 for the amplitude of the perturbation quantities is chosen. The Fig. 4 presents the results for  $\phi$  versus  $z$  for  $x = y = t = 0$ . Solid line corresponds to  $T = L = 0$  and  $C = 0.357$ . Dotted line corresponds to  $T = 2$ ,  $L = 0$ , and  $C = 0.343$ . Dashed line corresponds to  $T = 0$ ,  $L = 0.04$ , and  $C = 0.356$ . Dash-dot-dot line corresponds to  $T = 2$ ,  $L = 0.04$ , and  $C = 0.368$ . It can be seen from this figure that for the inertial and rotating case  $\phi$  is less negative as compared with the other cases, and its magnitude is smaller than that for the non-rotating counterpart over the lower-half of the layer. In addition, average value of  $|\phi|$  over the vertical depth of the layer for the inertial and rotating case is smaller than the one for its non-rotating counterpart. In addition, our generated data for the oscillatory mode at a later time  $t = 3\pi/(2|\sigma_{11}|)$  indicated that  $\phi$  is positive everywhere, and its vertical-average value for the rotating case is larger than the one for the non-rotating counterpart. An important result uncovered by our calculated data for  $\phi$ , such as the one presented in the Fig. 4, is that the vertical average of the perturbation to the solid fraction for the oscillatory mode is less negative for the rotating and inertial cases. Hence, industrial crystal growers may find such result useful in growing higher quality alloy crystals.

We now present some linear results for both  $L = 0$  and  $L \neq 0$  cases that for  $L = 0$  can also serve as some corrections to the corresponding results in R03. In R03 some errors occurred only in the numerical calculation of the frequency where an approximate value of 3.14 and not a sufficiently exact value was used for  $\pi$ . The approximate value like 3.14 for  $\pi$  was found to be unsatisfactory only for cases, where the value of the frequency was sufficiently close to that of  $\pi$  corresponding to values of the composite parameter  $G_t$  less than about 0.61 in the absence of rotation. If the value of 3.14 is used for  $\pi$  in the numerical evaluation of the frequency, then more than one oscillatory mode may also be generated as was found in R03. One graph

**Fig. 4** Perturbation to solid fraction versus  $z$  for  $x = y = t = 0.0$ , and  $S = C$ . Here solid, dotted, dashed, and dash-dot-dot lines present, respectively, the cases of  $T = L = C - 0.357 = 0$ ,  $T - 2 = L = C - 0.343 = 0$ ,  $T = L - 0.04 = C - 0.356 = 0$ , and  $T - 2 = L - 0.04 = C - 0.368 = 0$

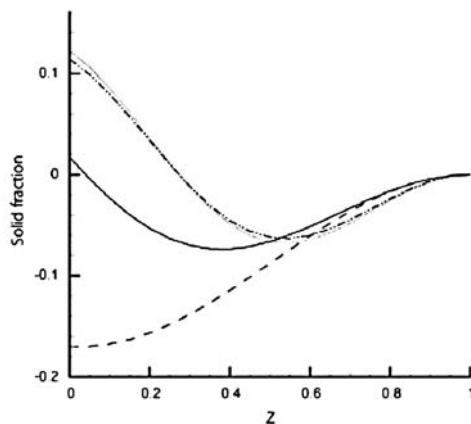
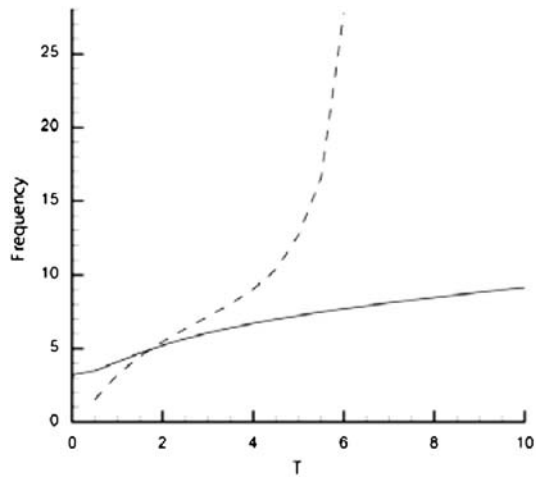


**Fig. 5**  $R_c$  versus  $T$  for  $G = 2$ ,  $G_t = 0.672$ , and  $K_1 = 1$ . Here solid and dashed lines present, respectively, the cases of  $L = 0$  and  $0.04$



in the Fig. 1 in R03, which was for the case  $G_t = 0.2$ , then need to be redrawn (see the solid line in Fig. 5 of the present paper) since it is not expected to be accurate at least for  $T = 0$ , even though the qualitative results presented in R03 for this figure remain unchanged. Figure 5 in the present paper shows frequency versus  $T$  for  $G = 2$  and  $G_t = 0.672$ , where the solid and dashed lines correspond, respectively, to  $L = 0$  and  $0.04$ . Frequency calculations in the present paper are done based on the sufficiently exact value of  $\pi$  ( $\pi = 3.141592654$ ). We have chosen the value of  $0.672$  for  $G_t$  since it corresponds to value of  $3.18$  for the frequency in the absence of rotation, which is the same value for the frequency for  $T = 0$  used in the graph in the Fig. 1 of R03. Figure 5 in the present paper also shows the dashed-line graph for the frequency versus  $T$  for  $L = 0.04$ . It can be seen from this graph that for the inertial case the period of the flow oscillation can be quite different from the one in the absence of the inertial effect. This figure also shows that for the given values of the parameters  $G$  and  $G_t$ , the period of the flow oscillation for  $L=0.04$  is larger (smaller) than that for  $L = 0$  if  $T < (>)T_1$ , where  $T_1$  is a value between  $1.5$  and  $2$ . The graph for  $L = 0.04$  has apparently an asymptote for  $T = T_2$ , where  $T_2$  is a value between  $6$  and  $6.5$ . For  $T > T_2$ , there is no non-zero frequency for  $L = 0.04$ ,  $G = 2$ , and  $G_t = 0.672$ . Finally it should be noted that in the non-inertial work presented in R03 the main qualitative results about the critical oscillatory mode, where  $G > 1$  and  $[G_t(\pi^2 + a^2)/(2\pi^2)] > 0.61$ , remain unchanged. This later condition on  $G_t$  is derived easily from a simple analogy between the rotating and non-rotating versions of (11b) and our finding that in the non-rotating case, where  $a = \pi$ , the value of  $\pi = 3.14$  used in the calculation is satisfactory if  $G_t > 0.61$ .

#### 4 Conclusion

We investigated the problem of effect of inertial force on linear oscillatory flow instabilities in a horizontal dendrite layer during the alloy solidification and uniformly rotating about the vertical axis. The interaction between the local solid fraction and the flow associated with the Coriolis term in the extended momentum-Darcy equation

is fully taken into account to determine the results. Over an extensive range of the parameter values, the inertial effect was found to reduce the domain for the presence of the oscillatory flow, while rotational effect enhances such domain. For sufficiently large rate of rotation and for given values of the other parameters no oscillatory flow is possible if inertial effect is present. Depending on the parameter values, there is a critical value of the rate of rotation below which the period of oscillation for the flow in the presence of the inertial effect is higher than that in the absence of the inertial force, while for the rate of rotation above its critical value the period of oscillation in the presence of inertial effect is smaller than that in the absence of the inertial effect. The oscillatory mode was found to be able to reduce the tendency for the chimney formation in the rotating dendrite layer. The effect of interaction between the local volume fraction of solid and the flow associated with the Coriolis term was found to be stabilizing.

## References

- Amberg, G., Homsy, G.M.: Nonlinear analysis of buoyant convection in binary solidification with application to channel formation. *J. Fluid Mech.* **252**, 79–98 (1993)
- Anderson, D.M., Worster, M.G.: A new oscillatory instability in a mushy layer during the solidification of binary alloys. *J. Fluid Mech.* **307**, 245–267 (1996)
- Chandrasekhar, S.: *Hydrodynamic and Hydromagnetic Stability*. Oxford University Press, Oxford (1961)
- Govender, S., Vadasz, P.: Weak nonlinear analysis of moderate Stefan number oscillatory convection in rotating mushy layers. *Transport Porous Med.* **48**, 353–372 (2002)
- Guba, P., Boda, J.: The effect of uniform rotation on convective instability of a mushy layer during binary alloys solidification. *Studia Geoph. Et Geod.* **42**, 289–296 (1998)
- Riahi, D.N.: On stationary and oscillatory modes of flow instability in a rotating porous layer during alloy solidification. *J. Porous Med.* **6**, 177–187 (2003)
- Vadasz, P.: Coriolis effect on gravity-driven convection in a rotating porous layer heated from below. *J. Fluid Mech.* **376**, 351–375 (1998)
- Worster, M.G.: Natural convection in a mushy layer. *J. Fluid Mech.* **224**, 335–359 (1991)
- Worster, M.G.: Instabilities of the liquid and mushy regions during solidification of alloys. *J. Fluid Mech.* **237**, 649–669 (1992)